https://doi.org/10.5194/gmd-2022-111
Preprint. Discussion started: 17 June 2022

Geoscientific Model Development
Discussions
Open Access
EGU

Advancing Precipitation Prediction Using a New Generation Storm-resolving Model Framework - SIMA-MPAS (V1.0): a Case Study over the Western United States

Xingying Huang*, Andrew Gettelman, William C. Skamarock, Peter Hjort Lauritzen, Miles Curry, Adam Herrington, John T. Truesdale, Michael Duda

Affiliation: National Center for Atmospheric Research, Boulder, CO 80305, USA

Correspondence to: Xingying Huang (xyhuang@ucar.edu)

Abstract: Global climate models (GCMs) have advanced in many ways as computing power has allowed more complexity and finer resolution. As GCMs reach storm-resolving scale, for predictions to be useful, they need to be able to produce realistic precipitation distributions and intensity at fine scales. This study uses a state-of-art storm-resolving GCM, the System for Integrated Modeling of the Atmosphere (SIMA), as the atmospheric component of the open-source Community Earth System Model (CESM) and a non-hydrostatic dynamical core - the Model for Prediction Across Scales (MPAS). For mean climatology, at uniform coarse (here, at 120km) grid-resolution, the SIMA-MPAS configuration is comparable to the standard hydrostatic CESM (with finite-volume (FV) dynamical core) with reasonable energy and mass conservation. We mainly investigate how the SIMA-MPAS model performs when reaching storm-resolving scale at 3km. To do this effectively, we compose a case study using a SIMA-MPAS variable resolution configuration with a refined mesh of 3km covering the western US and 60 km remaining of the globe. Our results show realistic representations of precipitation details over the refined complex terrains temporally and spatially. Along with much improved temperature features from well performed land-air interactions and realistic topography, we also demonstrate significantly enhanced snowpack distributions. We compared and evaluated the model performance using both observations and a traditional regional climate model. This work illustrates that a global SIMA-MPAS at storm resolving resolution can produce much more realistic regional climate variability, fine-scale features, and extremes to advance both climate and weather studies. The next-generation storm-resolving model could ultimately bridge large-scale forcing constraints and better-informed climate impacts and weather predictions across scales.

https://doi.org/10.5194/gmd-2022-111
Preprint. Discussion started: 17 June 2022

Geoscientific Model Development Discussions

1 Introduction

Climate models have advanced in many ways in the last decade including their atmospheric dynamical core and parameterization components. Given the recent development of Earth system model frameworks and advances in computer power, it is feasible to couple non-hydrostatic dynamical cores into global models allowing 'storm-resolving' scale on the order of a few kilometers (Satoh et al., 2019). These GSRMs (Global Storm-Resolving Models) have been constructed at a number of modeling centers (Satoh et al., 2019; Stevens et al., 2019; Dueben et al., 2020, Stevens et al., 2020, Caldwell et al., 2021). We expect an emerging trend in improving and applying the new modeling structures and platforms for a better and more accurate understanding of global and regional climate studies and weather-scale predictions.

The Community Earth System Model (CESM), one of the leading Earth system models, has been used in a wide range of climate studies. For high-resolution CESM applications, variable-resolution CESM-SE (spectral element core) for regional climate modeling has been used in many regional climate studies (such as Huang et al., 2016; Gettelman et al., 2018; Gettelman et al., 2019). More recently for storm-resolving modeling development, over the past decade there have been two efforts to bring the dynamical core from the Model for Prediction Across Scales (MPAS) into CESM. The first effort involved implementing the hydrostatic atmospheric dynamical core in MPAS Version 1 in the Community Atmosphere Model (CAM), which is the atmospheric component of CESM. This effort made available the horizontal variable-resolution mesh capability of the MPAS spherical centroidal Voronoi mesh (Ringler et al., 2010), and led to a number of studies (e.g., Rauscher et al., 2013).

Later, the static port of MPAS to CAM was updated with the nonhydrostatic MPAS atmospheric solver (Skamarock et al., 2012; Skamarock et al., 2014) to provide nonhydrostatic GSRM capabilities to CAM (Zhao et al., 2016). Neither of these ports was formally released, and the nonhydrostatic MPAS was not energetically consistent with CAM physics, or its energy fixer given, among other things, the height vertical coordinate used by MPAS. Furthermore, the MPAS modeling system and its dynamical core, being separate from CESM, have evolved from these earlier ports. To address the issues in the earlier MPAS dynamical core ports to CAM/CESM, the MPAS nonhydrostatic dynamical core has been brought into CAM/CESM as an external component, i.e., it is pulled from the MPAS development repository when CAM is built, and all advances in MPAS are immediately available to CESM-based configurations using MPAS. This latest port was accomplished as part of the SIMA (System for Integrated Modeling of the Atmosphere) project. Importantly, this implementation also includes an energetically consistent configuration of MPAS, with its height vertical coordinate, the CAM hydrostatic-pressure coordinate physics and the CAM energy fixer.

https://doi.org/10.5194/gmd-2022-111
Preprint. Discussion started: 17 June 2022

Geoscientific Model Development
Discussions

The MPAS dynamical core solves the fully compressible nonhydrostatic equations of motion and continues to be developed and used in many studies (Feng et al., 2021; Lin et al., 2022; and see https://mpas-dev.github.io/atmosphere/atmosphere.html). In this work, we test the storm-resolving capabilities in this new atmospheric simulation system. We use SIMA capabilities to configure a version of CESM with the MPAS nonhydrostatic dynamical core, called SIMA-MPAS instead of CESM-MPAS, since it is coupled only to a land model, with the other climate-system components being data components. In particular, we'd like to answer the question: can a non-hydrostatic dycore coupled global climate model reproduce observed wet season precipitation over targeted refinement regions? In addition, will this new development and modeling framework perform better or worse than a mesoscale model at similar resolution?

We aim to understand how this new SIMA-MPAS model configuration performs when configured for storm-resolving (convection permitting) scale for precipitation prediction over the western United States (WUS). Leveraging the recent significant progress in SIMA-MPAS development, we have undertaken experiments to understand the performance of SIMA-MPAS in precipitation simulations involving heavy storm events and relevant hydroclimate features at fine scales. We also explore large-scale dynamics and moisture flux transport over the subtropical region across the North Pacific. We evaluate the model results compared to both observations and a regional climate model. Employing the recent modeling developments in CESM with the MPAS dycore, the ultimate goal of this study is to evaluate the potential improvements to our understanding of atmospheric processes and prediction made possible with GSRM capabilities. We begin in section 2 with a description of the model configurations and experiments. Section 3 describes the main results, including mean climatology diagnostics, precipitation statistics and features, snowpack statistics features, and large-scale moisture flux and dynamics. A summary and discussion follow in Section 4.

2 Methods, experiments, and dataset

2.1 Methods and experiments

As briefly mentioned in the introduction section, we configure CESM2 (Danabasoglu et al., 2020) with the MPAS nonhydrostatic dynamical core and CAM6 physics. We call this configuration SIMA-MPAS. SIMA is a flexible system for configuring atmospheric models inside of an Earth System Model for climate, weather, chemistry and geospace applications (https://sima.ucar.edu). The components of this particular configuration also include the coupled land model CLM5 (with MOSART river model) and prescribed SST and ice. MPAS-Atmosphere employs a horizontal unstructured centroidal Voronoi tessellation (CVT) with a C-grid staggering (Ringler et al., 2010), and its numerics exactly conserve mass and scalar mass. Both horizontal uniform meshes and variable resolution meshes with smooth resolution transitions are available for MPAS-

https://doi.org/10.5194/gmd-2022-111
Preprint. Discussion started: 17 June 2022

Atmosphere, and this study employs both mesh types. It uses a hybrid terrain-following height coordinate (Klemp 2011).

We summarize here the key developments on the coupling of MPAS dynamical core to CAM physics and changes to CAM physics to accommodate MPAS. Most of all, we'd like to point out that a consistent coupling of the MPAS dynamic core with the CAM physics package is not trivial for several reasons. 1) MPAS uses a height (z) based vertical coordinate whereas CAM physics uses pressure. 2) The CAM physics package enforces energy conservation by requiring each parameterization to have a closed energy budget under the constant pressure assumption (Lauritzen et al., 2022). For the physics-dynamics coupling to be energy consistent (i.e., not be a spurious source/sink of energy) requires the energy increments in physics to match the energy increments in the dynamical core when adding the physics tendencies to the dynamics state. When "mixing" two vertical coordinates, that becomes non-trivial. 3) The prognostic state in MPAS is based on a modified potential temperature, density, winds, and dry mixing ratios whereas CAM uses temperature, pressure, winds and moist mixing ratios for the water species. The conversion between (discrete) prognostic states should not be a spurious source/sink of energy either. 4) Lastly, the energy fixer in CAM that restores energy conservation due to updating pressure (based on water leaving/entering the column), as well as energy dissipation in the dynamical core and physics-dynamics coupling errors (see Lauritzen and Williamson, 2019), assumes a constant pressure upper boundary condition. MPAS assumes constant height at the model top, so the energy fixer needs to use an energy formula consistent with the constant volume assumption. The details of the energy consistent physics-dynamics coupling and extensive modifications to CAM physics to accommodate MPAS are beyond the scope of this paper and will be documented in a separate source.

With the above significant progress in SIMA-MPAS development, we'd like to diagnose the performance of this new generation model when applied at convection-permitting resolutions and when bridging both weather and climate scale simulations in a single global model. We have chosen the WUS as our study region to examine the precipitation features in SIMA-MPAS at fine scales during wet seasons. We aim to figure out when the model outperforms and underperforms when compared to both observations and a traditional regional climate model at similar resolutions for mean and heavy precipitation behaviors. As mentioned in the introduction, we'd like to figure out whether a non-hydrostatic dycore coupled global climate model can reproduce observed wet season precipitation over targeted refinement regions. And will this new development and modeling framework perform better or worse than a mesoscale model at similar resolution?

To answer those questions, we have designed and conducted a set of experiments as shown in Table 1. In detail:

- Set A: We have tested CESM2 at the same coarse resolution using both MPAS (at 120km) as the non-hydrostatic core and Finite Volume (Danabasoglu et al., 2020) (at ~1 degree) as

https://doi.org/10.5194/gmd-2022-111
Preprint. Discussion started: 17 June 2022

the hydrostatic core for multiple years of climatology to get five-year mean F2000 climatology at ~1° for both MPAS and FV (finite-volume) dycore;

- Set B: as the main focus for this work, a variable resolution mesh is configured with 3km refinement centered over western us as shown in Figure 1, for five wet-season simulations with 60-3km mesh (year 1999 to 2004; November to March; FHIST component set for historical forcings); atmosphere conditions initialized by Climate Forecast System Reanalysis (CFSR) reanalysis data;

- Set C: In addition, we have also configured uniform 60km simulations for two wet seasons in contrast to the 60-3km ones (year 2000 to 2002; November to March)

- Set D: Lastly, to accommodate the recent changes to the MG microphysics scheme, we have repeated one simulation at 60-3km resolution for the first wet-season (i.e. year 1999-2000) using MG3 with graupel (Gettelman et al., 2019) instead of MG2 (Gettelman and Morrison 2015) as in the Set B simulations.

All simulations have been conducted with 58 vertical levels up to 43 km. Set A also includes experiments using 32 vertical levels. The dynamic time-step for MPAS dycore is 20s (i.e., seconds) for 60-3km experiments with physics time-step set to 120s. For 120km the MPAS dynamic timestep is 900s and the physics timestep is 1800s. We have used the default radiation time step (1 hour). The average cost including writes and restarts is ~4K to 6K core-hour for one-day simulation with the scaling of the high-performance computing to be further improved. We'd like to acknowledge that model tuning is not performed.

Table 1: A series of experiments in this study with different configurations

Dycore/Model experiments	Component set	Grid spacing	Simulation time	Vertical level	Physics/dynamics timestep and microphysics
MPAS	F2000climo	120km	5 years	32L, 58L	1800s/900s, MG2
FV	F2000climo	~1degree	5 years	32L, 58L	1800s/1800s, MG2
MPAS	FHIST	60-3km	1999-2004, Nov. - March	58L	120s/20s, MG2
MPAS	FHIST	60-3km	1999-2000, Nov. - March	58L	120s/20s, MG3
MPAS	FHIST	60km	2000-2002	58L	900s/450s, MG2

https://doi.org/10.5194/gmd-2022-111
Preprint. Discussion started: 17 June 2022

Geoscientific Model Development Discussions
Open Access
EGU

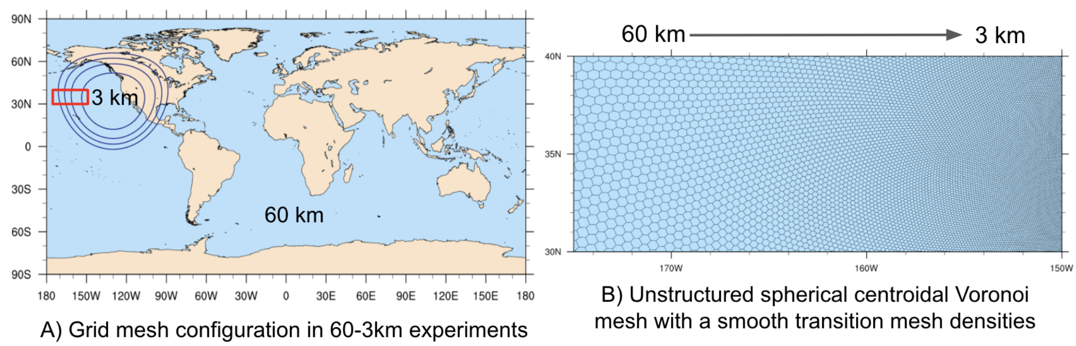

Figure 1: Grid mesh configuration in 60-3km experiments. A) The global domain mesh configuration with total grid columns of 835586; B) The zoomed-in region (see the red box depicted in panel A)) for the mesh structure from 60km to 3km.

2.2 Other datasets used in this study

In this work, we have employed observations from CERES EBAF products (Kato et al., 2018; Loeb et al., 2018) for cloud and radiation fluxes properties. We have used GHCN Gridded V2 CPC data (Fan and Van, 2008) for the land 2m air temperature globally, which is provided by the NOAA/OAR/ESRL PSL. We have also used PRISM data for gridded observed precipitation and temperature features (Daly et al., 2017) and Daymet data for gridded snow water equivalent reference (Thornton et al., 2020). Another important dataset used for comparison is the WRF 4km simulation data over CONUS from Rasmussen et al. (2021, https://rda.ucar.edu/datasets/ds612.5), which used the mean of the CMIP5 model as the boundary forcing. We extracted the same historical time data as the 60-3km simulations for direct evaluation (i.e., non-hydrostatic CESM as a vs. non-hydrostatic WRF as a widely used regional climate model). The topography details are shown in Figure 2 over the western US study region, showing that the complex terrains over coastal and mountainous regions have been well-resolved in SIMA-MPAS at 3km resolution (in contrast to 60km). This is comparable to the topography details in the WRF meso-scale model at a similar resolution.

https://doi.org/10.5194/gmd-2022-111
Preprint. Discussion started: 17 June 2022

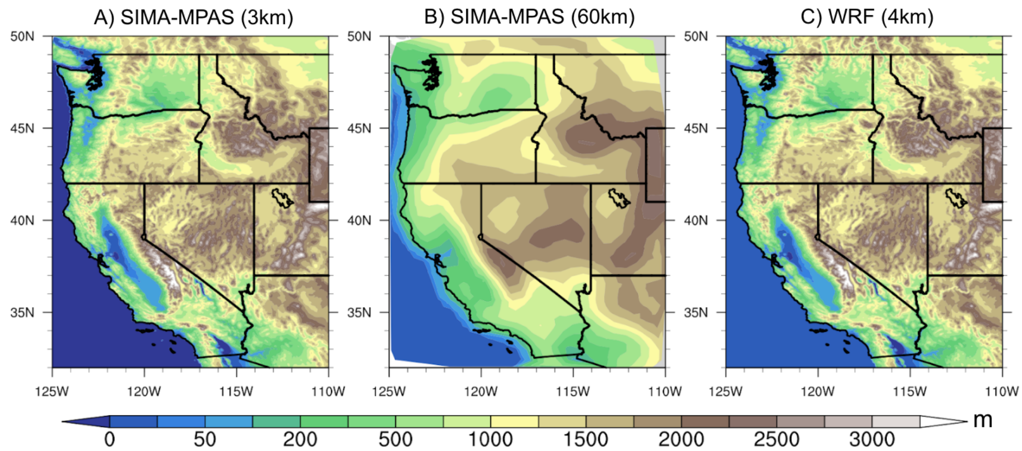

Figure 2: Topography over the Western US region. A) SIMA-MPAS at 3km refinement, B) SIMA-MPAS uniform 60km grid mesh, and C) WRF simulations at 4km over CONUS.

3 Results

3.1 Mean climatology diagnostics for CESM with MPAS dycore

As the non-hydrostatic dynamical core is coupled to CESM model framework, we'd like to understand the mean climate in SIMA-MPAS and how that compares to a standard hydrostatic core (here, using FV), with the experiments described in Table 1. We evaluate the global context of the new formulation of CESM with a non-hydrostatic dynamical core with both 32 and 58 vertical levels. The 58 layer has higher resolution in the Planetary Boundary Layer (PBL) and in the mid and upper troposphere (about 10 additional levels in the PBL and decreasing vertical grid spacing from 1000m to ~500m near the tropopause). Satellite observations are used for comparison as described in the above section 2.2. Simulations results are averaged over the climatological present day (year 2000) conditions with 5 years long.

https://doi.org/10.5194/gmd-2022-111
Preprint. Discussion started: 17 June 2022

Geoscientific Model Development
Discussions
Open Access
EGU

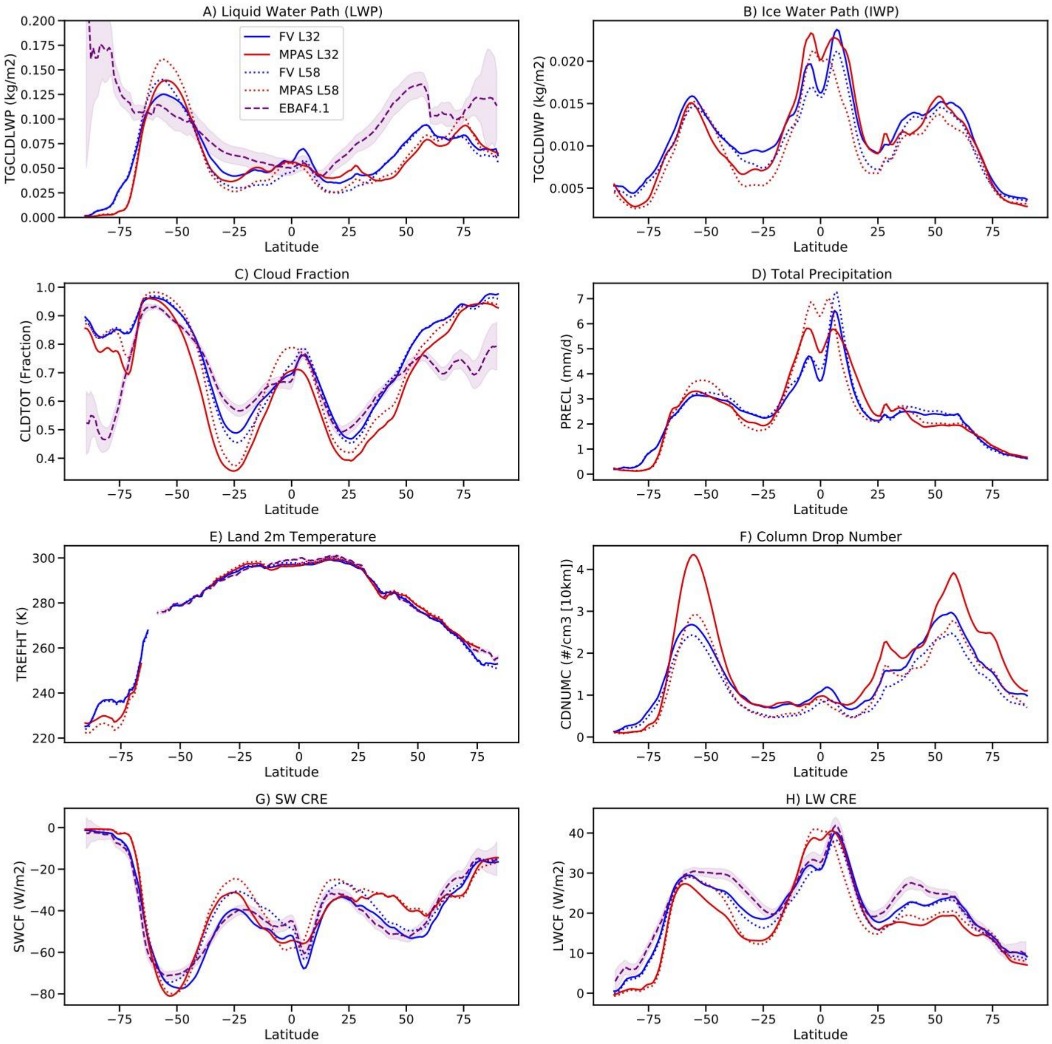

Figure 3: Zonal mean climatology from 5-year simulations with CESM2-CAM6. A) Liquid Water Path (LWP), B) Ice Water Path (IWP), C) Cloud Fraction, D) Total precipitation rate, E) Land 2m air Temperature, F) Column drop number, G) Shortwave Cloud Radiative Effect (SW CRE), H) Longwave (LW) CRE. Simulations are the default Finite Volume (FV) dynamical core with 32 levels (FV L32: Blue Solid) and 58 levels (FV L58: Blue Dashed). Also, the MPAS dynamical core with 32 levels (MPAS L32: Red Solid) and 58 levels (MPAS L58). Observations shown in Purple from CERES 20-year climatology from 2000-2020 for LWP, Cloud Fraction, SW CRE and LW CRE, and CPC surface temperature from 1990-2010 for E). Shaded values are 1 sigma annual standard deviations.

https://doi.org/10.5194/gmd-2022-111
Preprint. Discussion started: 17 June 2022

Figure 3 indicates that MPAS simulations have a very similar climate to FV simulations. There are some differences in tropical ice water path in the southern hemisphere tropics, and some significant differences in sub-tropical cloud fraction. The climate differences between 32 and 58 levels are also similar between dynamical cores: decreases in liquid and ice water path at higher vertical resolution. SIMA-MPAS has slight increases in cloud fraction and precipitation at higher vertical resolution, while SIMA-FV has little change or slight decreases in cloud fraction. Land surface temperature is well reproduced when ocean temperatures are fixed with both dynamical cores. Column drop number with CAM-MPAS is lower than CAM-FV, but more stable with respect to resolution changes. Subtropical SW CRE and LW CRE have higher magnitudes with CAM-MPAS, consistent with higher LWP and cloud fraction in these regions, yielding better agreement with the meridional CRE structure.

Analysis of the atmospheric wind and temperature structure (Figure S1 and Figure S2) indicates that SIMA-MPAS compares as well or better to reanalysis winds and thermal structure in the vertical as SIMA-FV. Overall, SIMA-MPAS produces a reasonable climate simulation, with biases relative to observations that are not that different from SIMA-FV simulations, despite limited adjustments being made to momentum forcing. SIMA-MPAS has a realistic zonal wind structure with sub-tropical tropospheric and polar stratospheric jets. There are differences in magnitude from ERAI, but MPAS (which has not been fully tuned) produces a realistic wind distribution. For the temperature profile, there are patterns of bias between the high and low latitudes indicating different stratospheric circulations between the model and the reanalysis. That could be adjusted with the drag and momentum forcing in the model. Note that no adjustment of the physics has been performed.

3.2 Precipitation distribution and statistics

3.2.1 Mean precipitation features

In the Western US during the wet season (Nov-Mar), most of the precipitation occurs over the coastal ranges and mountainous regions, with significant impacts on both water resources and potential flood risk management (Hamlet and Lettenmaier, 2007; Dettinger et al., 2011; Huang et al., 2020a). In Figure 4, we show the wet season mean precipitation features over the targeted region with differences from observations. The result demonstrates that SIMA-MPAS can well simulate the precipitation intensity and spatial distributions, as compared to PRISM observations. The spatial features are well captured with the spatial correlation of about 0.93 with precipitation mainly distributed over the Cascade Range, Coastal Range, Sierra Nevada, and the Rocky Mountains. If looking at the precipitation at the coarser resolution (60km, Figure S3a) in SIMA-MPAS, the mean domain-average of the precipitation (for about 2.43 mm, when averaged over years 2000-2002) is similar to the fine resolution results (for about 2.61 mm) but lacking important regional variability and spatial textures.

https://doi.org/10.5194/gmd-2022-111
Preprint. Discussion started: 17 June 2022

In terms of biases, SIMA-MPAS 3km overall underestimates the precipitation by about 0.07 mm (bias averaged over the plotted domain), especially over the windward regions. WRF, on the other hand, tends to overestimate the precipitation in most regions (for about 0.53 mm, bias averaged over the plotted domain)) except for the northwest coast and some Rocky Mountains regions, which can be seen from the relative difference plot (Figure 4c). The relative differences in precipitation are generally large over the dryer regions in SIMA-MPAS. Overall, the bias is negative (for about -0.81 mm on average) over windward regions, but positive over the lee side (for about 0.48 mm on average). We also notice that the precipitation texture is relatively smoothed over the Rocky Mountains resulting in a large underestimation bias, which could be due to the fact that the boundary for the 3km mesh grids is nearing those regions (see Figure 1). This can also be told from the smoother topography over the 3km mesh bounds and transient domains (see Figure 2). For future regional refined applications, we would suggest having a reasonably larger domain area than the study region at the finest resolution to accommodate the noise and instability from mesh transition.

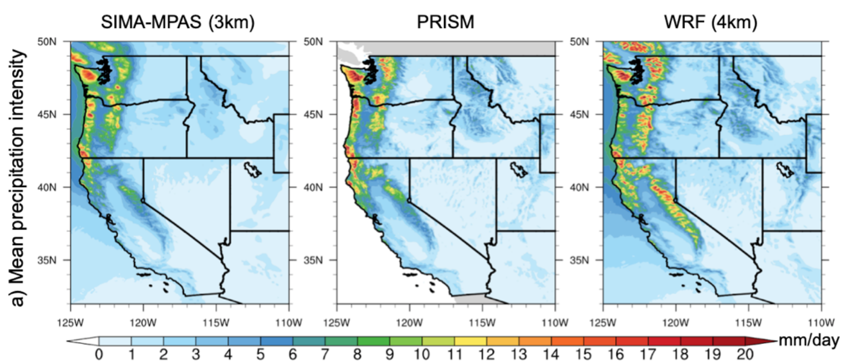

https://doi.org/10.5194/gmd-2022-111
Preprint. Discussion started: 17 June 2022

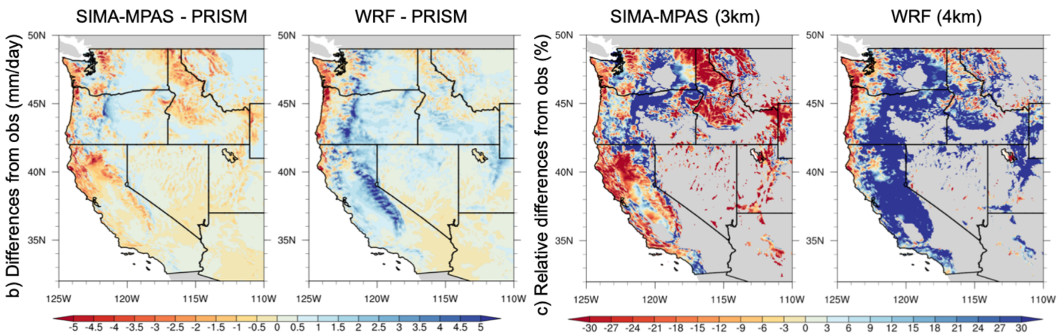

Figure 4: Mean simulated precipitation and differences from observation: a) Wet-season (Nov-March) daily precipitation intensity over western US (1999-2004); b) Absolute differences from PRISM reference; c) Similar as b, but for relative differences from PRISM (grid box values less than 1mm/day have been masked)).

Over the Western US, especially in the coastal States, heavy precipitation can be induced by extreme storm events mainly in the form of atmospheric rivers (Leung and Qian, 2009; Neiman et al., 2011; Rutz et al., 2014; Ralph et al., 2019; Huang et al., 2020b). The capability to capture and predict such extreme events is a significant part of the application of weather and climate models (Meehl et al., 2000; Sillmann et al., 2017; Bellprat et al., 2019). To figure out the performance of SIMA-MPAS in reproducing the precipitation frequency distribution, we combine all the daily data from all the grid points at each coastal State (California, Oregon, and Washington) to calculate the frequency of daily precipitation by intensity (Figure 5). SIMA-MPAS captures the distribution of precipitation intensity with respect to PRISM observations quite well, even better than WRF, particularly at more extreme values. And this finding is consistent across all the three regions.

When looking at the precipitation days with intensity less than 10 to 15 mm/day, SIMA-MPAS shows a close match to PRISM data, while WRF tends to underestimate the probability. For more extreme precipitation days, models tend to diverge in terms of the behaviors with SIMA-MPAS showing some underestimation over California and Washington regions (for average of ~14%, ~7% and ~18% bias for days when intensity exceeds 20 mm/day and less than 60 mm/day for California, Oregon, and Washington respectively). WRF generally overestimates the heavy precipitation frequency to a much larger extent (for an average bias of ~42%, ~51% and ~18% for California, Oregon, and Washington respectively). The sign of the biases is consistent with the previously discussed mean precipitation biases. We do acknowledge that the initialization without nudging conditions does not get the monthly or higher time variability but is able to get the seasonal means and distributions. The results further testify the capability of using SIMA-MPAS for precipitation studies, giving us good confidence in using SIMA-MPAS for storm events studies.

https://doi.org/10.5194/gmd-2022-111
Preprint. Discussion started: 17 June 2022

Geoscientific Model Development
Discussions
Open Access
EGU

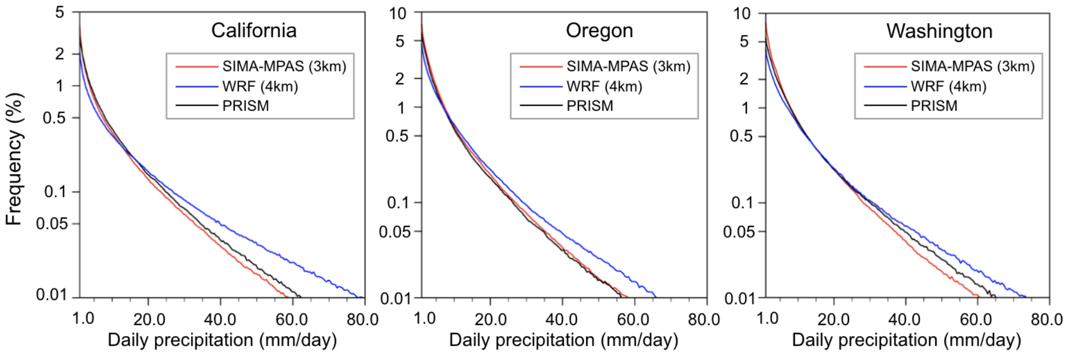

Figure 5: Probability distribution of daily precipitation frequency. All the daily datasets from the five wet seasons for all grid points in each State are used to construct the distribution statistics. The blue lines refer to WRF reference data, the black lines are for the PRISM observation and the SIMA-MPAS results are in red-colored lines. The x-axis starts from 1mm/day and the y-axis is transformed with a logarithmic scaling for better visualization of the upper tail distribution.

3.2.2 MG2 vs. MG3 microphysics for simulated precipitation in SIMA-MPAS

We'd like to point out that we have used the default microphysics scheme-MG2 (Gettelman et al., 2015) when configuring those experiments from the CESM2 model. We acknowledge that MG3 (including rimed ice, graupel in this case) could be a better option here with the rimed hydrometeors added to the MG2 version (see Gettelman et al., 2019) especially when pushing to mesoscale simulations and for orographic precipitation. To fulfill this caveat but still make the best use of current simulation data, another experiment using the MG3 microphysics scheme was added for the first wet season (1999-2000). Similar diagnostics have been performed as in the previous part but for the results from this one wet season only (as shown in Figure 6).

We do notice that using only one season, although still outperforming WRF output, SIMA-MPAS shows a larger bias from the observation with more notable underestimations for mean intensity and frequency distributions. MG3 microphysics produces stronger precipitation than the MG2 version and the results match better the observation for both spatial mean and frequency distribution. Due to the seasonal and interannual variability, we still need to investigate more different cases, and it is our next-step plan to further investigate the model performance with more testbeds.

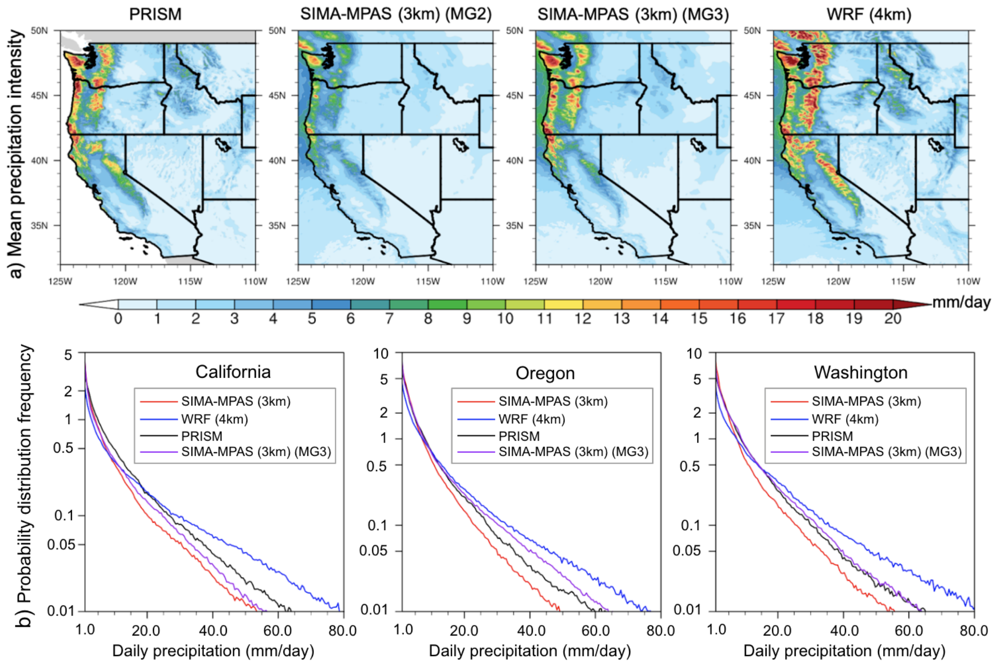

Figure 6: MG2 vs. MG3 microphysics used in SIMA-MPAS for the wet-season (Nov-March) precipitation over western US (1999-2000). a) mean precipitation intensity; b) Probability distribution of daily precipitation frequency, like Figure 5 but for only one wet season with SIMA-MPAS (MG3) added in purple lines.

3.3 Snowpack statistics features

As we know, snowpack representation has remained a long-standing issue in climate models due to the complicated land-atmosphere interactions and its sensitivities in thermal and hydrological properties (DeWalle & Rango 2008; Liu et al., 2017; Kapnick et al., 2018). It is one of our targets that with improved precipitation and temperature presentation over much better-resolved complex mountainous terrains, the snowpack features can be better represented in CESM. Here, we have compared the accumulated snow water equivalent (SWE) results, which refer to the total accumulated snow from mid-Nov to mid-March (based on daily output), and then averaged over the five seasons (see Figure 7). By comparing the gridded snow water equivalent reference data (Daymet), it shows that SIMA-MPAS (MG2) can produce good estimates of the snowpack over the mountainous regions and even better than WRF simulations (which is related to its precipitation overestimation). Overall, SIMA-MPAS does a good job in retrieving the spatial details for snowpack distribution over mountainous regions (mainly over the Cascade Range, Coastal Range, Sierra Nevada, and the Rocky Mountains) with some positive bias over the northern Cascade Range.

https://doi.org/10.5194/gmd-2022-111
Preprint. Discussion started: 17 June 2022

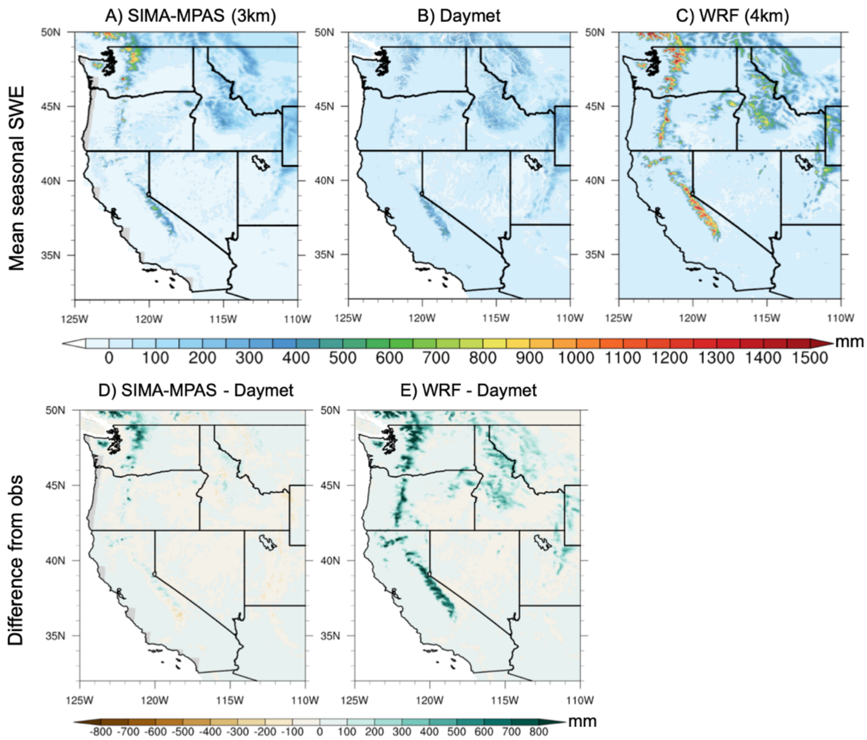

Figure 7: Wet-season (Nov. till March) snow water equivalent (SWE) over western US (1999-2004). First row: Seasonal mean SWE from A) SIMA-MPAS, B) Daymet observation, and C) WRF data; Second row: Absolute differences from Daymet.

As the snowfall is dominated by the near-surface temperature and precipitation values, we have examined the 2m temperature (T2) here to see how well temperature is captured in SIMA-MAPS. In Figure 8, the mean T2 (T2mean) is shown averaged over all simulated wet seasons. In general, near-surface temperature results from SIMA-MPAS are overall matched with observations across varied climate zones including coastal areas, agriculture, desert regions, inland and mountainous. However, we also notice that SIMA-MPAS tends to be warmer over most places (with the averaged bias of about 0.65°C over the plotted domain), except over very high mountain top ranges with cooler bias. On average, the difference for the regions with warmer biases is about 1.35°C and the difference for those areas with cooler biases is about -0.99°C when compared to PRISM data. On the contrary, WRF tends to be cooler in most regions except the southern part of Central Valley and some desert regions in the southwest US (the average bias is about -1.84°C over the plotted domain). We have also investigated the T2 bias in the 120km simulations to see if this is a consistent model bias. By comparing FV and MPAS together (Figure S4), it turns out that SIMA-MPAS tends to be warmer with higher net surface shortwave and longwave fluxes over the wet-

https://doi.org/10.5194/gmd-2022-111
Preprint. Discussion started: 17 June 2022

Geoscientific Model Development Discussions
Open Access

season period discussed here (Figure S5). Still, overall, the land model coupled with the atmosphere also does a good job here under a realistic topography. Given the well-capture precipitation and a reasonably coupled land model, it seems to be promising to better predict the hydroclimate change using a unified non-hydrostatic climate model.

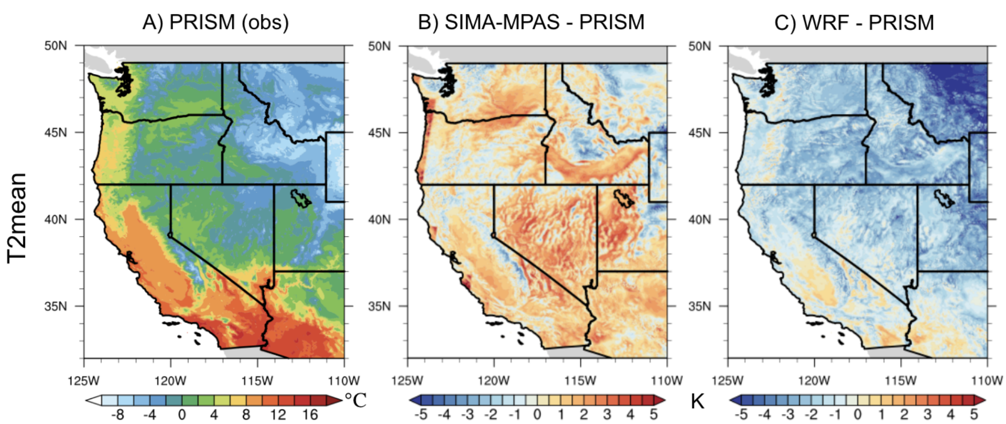

Figure 8: Daily mean 2m air temperature (T2mean) averaged over (1999-2004, Nov-March). A) PRISM observation dataset; B) and C) The differences between SIMA-MPAS and WRF from PRISM respectively; (Note: for difference plot, all data are regridded to the same resolution as PRISM).

3.4 Large-scale moisture flux and dynamics

For further investigation, we have investigated the wind profile that directly connects to the subtropical to middle latitudes moisture fluxes over the northeast Pacific and the hitting western US regions. First, we have examined the vertical wind patterns (at 130˚W, near the Western US coast) at both 60-3km and 60km to determine the dynamic changes with the refinement mesh (Figure 9). As we can see, the mean westerly zonal winds are about 10% stronger at the jet stream level near 200-250hPa in 60-3km simulations compared to the 60km results. The mean meridional wind (dominantly southward) however is weaker in 60-3km simulations than the 60km ones. The precipitation over the western US coast is largely associated with the concentrated water vapor transport over the North Pacific, known mainly in the form of atmospheric rivers (Rutz et al., 2014). It is our further interest to investigate the wind dynamics transitioning from coarse scale to mesoscale in future work. Another source of the precipitation uncertainty we'd like to acknowledge could be from the physics timestep (see Figure S6) when comparing the precipitation in 60-3km simulations (a shorter physics time-step) to the 60km results at the regions with the same grid resolutions.

https://doi.org/10.5194/gmd-2022-111
Preprint. Discussion started: 17 June 2022

Geoscientific Model Development
Discussions

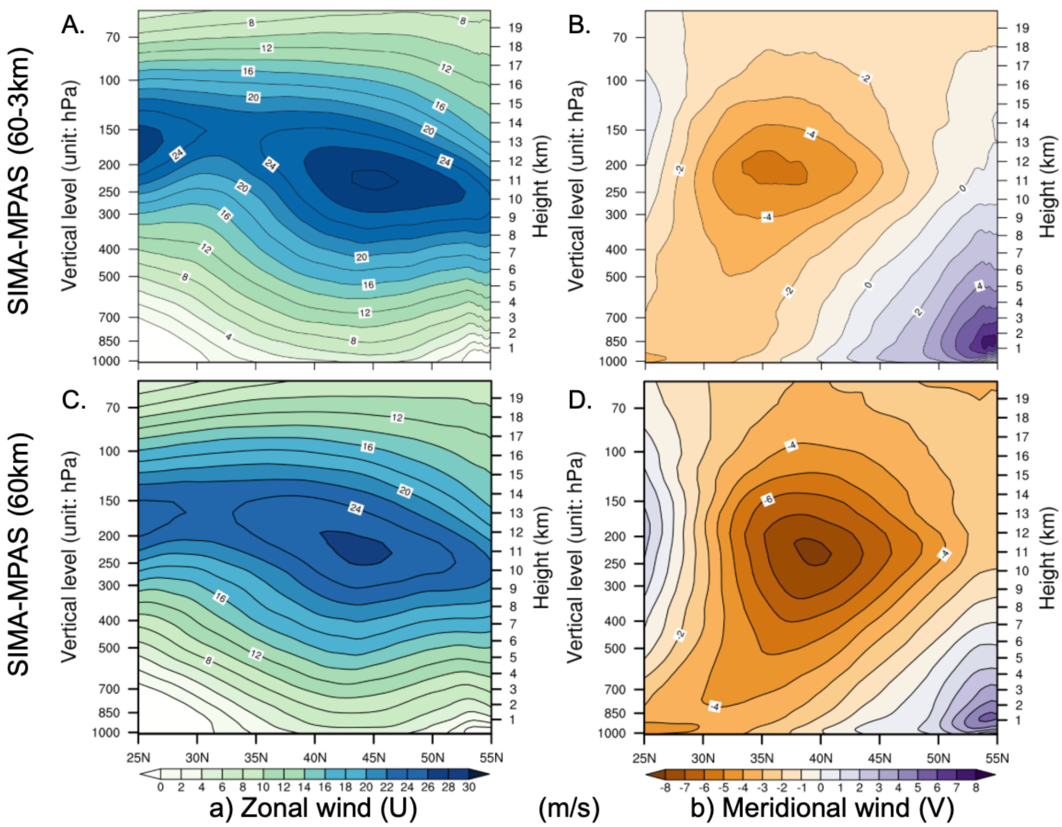

Figure 9: Composite wind profile along western US coast (cross-section at 130W, near the western US coast) (averaged over 2000-2002, Nov-March). a) Mean latitude-height cross-section of zonal winds (m/s) for SIMA-MPAS 60-3km (panel A) and 60km (panel C); b) similar as a), except for meridional winds (panel B and D).

When we look at those global simulations with refined regions, we can figure out the large-scale moisture flux patterns. In Figure 10, we show the integrated water vapor transport from both the simulations with and without regional refinement. Largely controlled by the zonal winds (as also in Figure 9), the spatial pattern of the moisture flux is generally similar between those two sets of experiments. When calculating the IVT values 130˚W with the regridded data, the differences are minor along the WUS latitudes (for about 3% on average). In general, the large-scale dynamics and fine-scale processes in local regions reach a good synthesis in a non-hydrostatic global climate model as developed and configured in this study to well represent and potentially to powerfully predict the precipitation features either at the weather or climate scales.

https://doi.org/10.5194/gmd-2022-111
Preprint. Discussion started: 17 June 2022

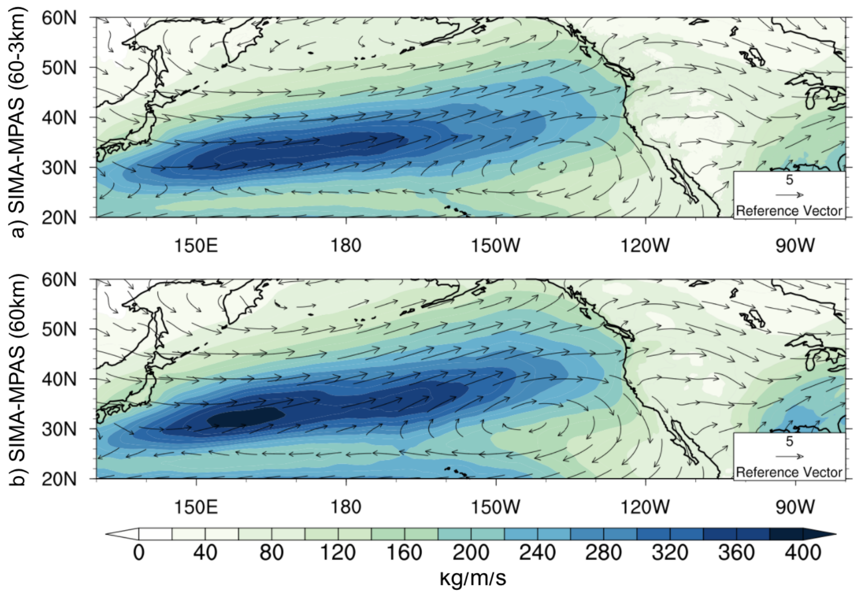

Figure 10: Mean instantaneous vertically integrated water vapor flux transport over western US (2000-2002, Nov-March): a) SIMA-MPAS 60-3km and b) SIMA-MPAS 60km. Wind is overlaid for the averaged lower levels (height from ~500m to ~2000m).

4 Summary and discussion

In this study, we describe SIMA-MPAS, which is built upon the open-source Community Earth System Model (CESM) with a non-hydrostatic dynamical core, the Model for Prediction Across Scales (MPAS), we'd like to try to answer several questions about the performance of this new generation model when applying at convection-permitting resolutions and when bridging both weather and climate scale simulations in a single global model. We have chosen the western US as our study region to examine the precipitation features in SIMA-MPAS at fine scales and how the model performs when compared to both observations and a regional climate model.

To answer those questions, we have designed and conducted a set of experiments. First, we have tested CESM at the same coarse resolution using both MPAS as the non-hydrostatic core and finite-volume as the hydrostatic core for multiple years of climatology. Secondly, and, as the focus of this work, a variable resolution mesh is configured with 3km refinement centered over the western US. We have done five separate wet-season simulations to get the precipitation statistics. In addition, we have also included uniform 60km simulations from the model for two seasons.

We first evaluated the mean climate in SIMA-MPAS to see how that compares to the hydrostatic model counterpart (here, SIMA-FV). The diagnostics show that MPAS simulations have a very

https://doi.org/10.5194/gmd-2022-111
Preprint. Discussion started: 17 June 2022

similar climate to FV simulations. SIMA-MPAS has slight increases in cloud fraction and precipitation at the higher vertical resolution, while SIMA-FV has little change or slight decreases in cloud fraction. Overall, SIMA-MPAS produces a reasonable climate simulation, with biases relative to observations that are not that different from SIMA-FV simulations, despite limited adjustments being made to momentum forcing and no adjustment of the physics has been performed.

When compared to both observations and a traditional regional climate model at similar fine resolutions for mean and heavy precipitation behaviors, SIMA-MPAS did a pretty good job in capturing the spatial pattern and mean intensity in general, which is also comparable to WRF results. We do notice there are some underestimations in SIMA-MPAS and overestimations in WRF. SIMA-MPAS captures the distribution of precipitation intensity with respect to PRISM observations even better than WRF, particularly when going to more extreme values. And this finding is consistent across all the three coastal States. With additional experiments, SIMA-MPAS with MG3 microphysics (graupel) produces stronger precipitation than the MG2 version (as used in other experiments in this study as the default microphysics scheme) and the MG3 results match better the observation for both spatial mean and frequency distribution. We acknowledge that MG3 could be a better option here with the rimed hydrometeors added to the MG2 version (see Gettelman et al., 2019 for detailed descriptions) especially when pushing to mesoscale simulations and for orographic precipitation.

We also show that SIMA-MPAS can produce good estimates of the snowpack over the mountainous regions and is even better than WRF simulations (which is related to its precipitation overestimation). Overall, SIMA-MPAS does a good job in retrieving the spatial details for snowpack distribution over mountainous regions (mainly over the Cascade Range, coastal range, Sierra Nevada, and the Rocky Mountains) with some positive bias over the northern Cascade Range. We also notice that SIMA-MPAS tends to be warmer over most places, except over very high mountain top ranges with cooler bias. Overall, given the well-capture precipitation and a reasonably coupled land model, it seems to be promising to better predict the hydroclimate change using a unified non-hydrostatic climate model.

The results further testify the capability of using SIMA-MPAS for precipitation studies, giving us good confidence in using SIMA-MPAS for storm events studies. The large-scale dynamics and fine-scale processes in local regions reach a good synthesis in a non-hydrostatic global climate model as developed and configured in this study to well represent and potentially to powerfully predict the precipitation features either at the weather or climate scales. We do acknowledge that the initialization without nudging conditions does not get the monthly or higher time variability but is able to get the seasonal means and distributions. Therefore, it is key for this study to have multiple seasons' results to investigate the model performance in precipitation statistics instead. It is also our further interest to investigate the wind dynamics transitioning from coarse-scale to mesoscale in future work and to further investigate the model performance with more testbeds for convective-permitting weather and climate systems across scales.

Data and code availability: The data and codes used in this work is available for access from this DOI link: https://doi.org/10.5281/zenodo.6558578. The model used in this study can be downloaded from the open-shared link: https://github.com/ESCOMP/CAM.

Author Contributions: XH and AG designed the study and the experiments. All authors contributed to the work in the model development. XH performed the simulations with assistance from AG, MC, WS, PL and AH. XH and AG contributed to the investigation and visualization. XH prepared the manuscript with review and edits from AG, WS, PL and AH.

Acknowledgments

We acknowledge the open-shared dataset used in this study including CERES EBAF products (https://ceres.larc.nasa.gov/data/), GHCN Gridded V2 CPC data provided by the NOAA/OAR/ESRL PSL (https://www.psl.noaa.gov/data/gridded/data.ghcncams.html), PRISM and Daymet observations, and WRF simulations at 4km (https://rda.ucar.edu/datasets/ds612.5/). We acknowledge the funding support from NSF funded project Earthworks (award number is NSF 2004973). We also acknowledge the partial support from the National Center for Atmospheric Research (NCAR), which is a major facility sponsored by the NSF under Cooperative Agreement 1852977, and the high-performance computing support and data storage resources from the Cheyenne supercomputer (doi:10.5065/D6RX99HX) provided by the Computational and Information Systems Laboratory (CISL) at NCAR.

Competing Interest Statement: The authors have no competing interests to declare.

References

Bellprat, O., Guemas, V., Doblas-Reyes, F. and Donat, M.G., 2019. Towards reliable extreme weather and climate event attribution. Nature communications, 10(1), pp.1-7.

Caldwell, P.M., Terai, C.R., Hillman, B., Keen, N.D., Bogenschutz, P., Lin, W., Beydoun, H., Taylor, M., Bertagna, L., Bradley, A.M. and Clevenger, T.C., 2021. Convection-Permitting Simulations With the E3SM Global Atmosphere Model. Journal of Advances in Modeling Earth Systems, 13(11), p.e2021MS002544.

Dettinger, M.D., Ralph, F.M., Das, T., Neiman, P.J. and Cayan, D.R., 2011. Atmospheric rivers, floods and the water resources of California. Water, 3(2), pp.445-478.

https://doi.org/10.5194/gmd-2022-111
Preprint. Discussion started: 17 June 2022

Dueben, P.D., Wedi, N., Saarinen, S. and Zeman, C., 2020. Global simulations of the atmosphere at 1.45 km grid-spacing with the Integrated Forecasting System. Journal of the Meteorological Society of Japan. Ser. II.

DeWalle, D.R. and Rango, A., 2008. Principles of snow hydrology. Cambridge University Press.

Fan, Y., and H. van den Dool (2008), A global monthly land surface air temperature analysis for 1948-present, J. Geophys. Res., 113, D01103, doi:10.1029/2007JD008470.

Feng, Z., Song, F., Sakaguchi, K. and Leung, L.R., 2021. Evaluation of mesoscale convective systems in climate simulations: Methodological development and results from MPAS-CAM over the United States. Journal of Climate, 34(7), pp.2611-2633.

Gettelman, A., H. Morrison, S. Santos, P. Bogenschutz, and P. M. Caldwell. "Advanced two-moment bulk microphysics for global models. Part II: Global model solutions and aerosol–cloud interactions." Journal of Climate 28, no. 3 (2015): 1288-1307.

Gettelman, A., Callaghan, P., Larson, V.E., Zarzycki, C.M., Bacmeister, J.T., Lauritzen, P.H., Bogenschutz, P.A. and Neale, R.B., 2018. Regional climate simulations with the community earth system model. Journal of Advances in Modeling Earth Systems, 10(6), pp.1245-1265.

Gettelman, A., Morrison, H., Thayer-Calder, K. and Zarzycki, C.M., 2019. The impact of rimed ice hydrometeors on global and regional climate. Journal of advances in modeling earth systems, 11(6), pp.1543-1562.

Goldenson, N., Leung, L.R., Bitz, C.M. and Blanchard-Wrigglesworth, E., 2018. Influence of atmospheric rivers on mountain snowpack in the western United States. Journal of Climate, 31(24), pp.9921-9940.

Hamlet, A.F. and Lettenmaier, D.P., 2007. Effects of 20th century warming and climate variability on flood risk in the western US. Water Resources Research, 43(6).

Huang, X., Rhoades, A.M., Ullrich, P.A. and Zarzycki, C.M., 2016. An evaluation of the variable-resolution CESM for modeling California's climate. Journal of Advances in Modeling Earth Systems, 8(1), pp.345-369.

Huang, X., Stevenson, S. and Hall, A.D., 2020a. Future warming and intensification of precipitation extremes: A “double whammy” leading to increasing flood risk in California. Geophysical Research Letters, 47(16), p.e2020GL088679.

Huang, X., Swain, D.L. and Hall, A.D., 2020b. Future precipitation increase from very high resolution ensemble downscaling of extreme atmospheric river storms in California. Science Advances, 6(29), p.eaba1323.

https://doi.org/10.5194/gmd-2022-111
Preprint. Discussion started: 17 June 2022

Kapnick, S.B., Yang, X., Vecchi, G.A., Delworth, T.L., Gudgel, R., Malyshev, S., Milly, P.C., Shevliakova, E., Underwood, S. and Margulis, S.A., 2018. Potential for western US seasonal snowpack prediction. Proceedings of the National Academy of Sciences, 115(6), pp.1180-1185.

Kato, S., F. G. Rose, D. A. Rutan, T. E. Thorsen, N. G. Loeb, D. R. Doelling, X. Huang, W. L. Smith, W. Su, and S.-H. Ham, 2018: Surface irradiances of Edition 4.0 Clouds and the Earth's Radiant Energy System (CERES) Energy Balanced and Filled (EBAF) data product, J. Climate, 31, 4501-4527, doi: 10.1175/JCLI-D-17-0523.1.

Klemp, J.B., 2011. A terrain-following coordinate with smoothed coordinate surfaces. Monthly weather review, 139(7), pp.2163-2169.

Leung, L.R. and Qian, Y., 2009. Atmospheric rivers induced heavy precipitation and flooding in the western US simulated by the WRF regional climate model. Geophysical research letters, 36(3).

Liu, C., Ikeda, K., Rasmussen, R., Barlage, M., Newman, A.J., Prein, A.F., Chen, F., Chen, L., Clark, M., Dai, A. and Dudhia, J., 2017. Continental-scale convection-permitting modeling of the current and future climate of North America. Climate Dynamics, 49(1), pp.71-95.

Lauritzen, P.H. and D. L. Williamson, 2019: A total energy error analysis of dynamical cores and physics-dynamics coupling in the Community Atmosphere Model (CAM): J. Adv. Model. Earth Syst., DOI:10.1029/2018MS001549.

Lauritzen, P.H. and co-authors, 2022: Reconciling and improving formulations for thermodynamics and conservation principles in Earth System Models (ESMs): J. Adv. Model. Earth Syst. (submitted; https://www.cgd.ucar.edu/cms/pel/papers/LetAl2022JAMES.pdf)

Lin, G., Jones, C.R., Leung, L.R., Feng, Z. and Ovchinnikov, M., 2022. Mesoscale convective systems in a superparameterized E3SM simulation at high resolution. Journal of Advances in Modeling Earth Systems, 14(1), p.e2021MS002660.

Loeb, N. G., D. R. Doelling, H. Wang, W. Su, C. Nguyen, J. G. Corbett, L. Liang, C. Mitrescu, F. G. Rose, and S. Kato, 2018: Clouds and the Earth's Radiant Energy System (CERES) Energy Balanced and Filled (EBAF) Top-of-Atmosphere (TOA) Edition-4.0 Data Product. J. Climate, 31, 895-918, doi: 10.1175/JCLI-D-17-0208.1.

Meehl, G.A., Zwiers, F., Evans, J., Knutson, T., Mearns, L. and Whetton, P., 2000. Trends in extreme weather and climate events: issues related to modeling extremes in projections of future climate change. Bulletin of the American Meteorological Society, 81(3), pp.427-436.

Neiman, P.J., Schick, L.J., Ralph, F.M., Hughes, M. and Wick, G.A., 2011. Flooding in western Washington: The connection to atmospheric rivers. Journal of Hydrometeorology, 12(6), pp.1337-1358.

https://doi.org/10.5194/gmd-2022-111
Preprint. Discussion started: 17 June 2022

Ralph, F.M., Rutz, J.J., Cordeira, J.M., Dettinger, M., Anderson, M., Reynolds, D., Schick, L.J. and Smallcomb, C., 2019. A scale to characterize the strength and impacts of atmospheric rivers. Bulletin of the American Meteorological Society, 100(2), pp.269-289.

Rasmussen, R., A. Dai, C. Liu, and K. Ikeda. 2021. CONUS (Continental U.S.) II High Resolution Present and Future Climate Simulation. Research Data Archive at the National Center for Atmospheric Research, Computational and Information Systems Laboratory. https://rda.ucar.edu/datasets/ds612.5/. Accessed on December 4, 2021.

Rauscher, S.A., Ringler, T.D., Skamarock, W.C. and Mirin, A.A., 2013. Exploring a global multiresolution modeling approach using aquaplanet simulations. Journal of Climate, 26(8), pp.2432-2452.

Ringler, T.D., Thuburn, J., Klemp, J.B. and Skamarock, W.C., 2010. A unified approach to energy conservation and potential vorticity dynamics for arbitrarily-structured C-grids. Journal of Computational Physics, 229(9), pp.3065-3090.

Rutz, J.J., Steenburgh, W.J. and Ralph, F.M., 2014. Climatological characteristics of atmospheric rivers and their inland penetration over the western United States. Monthly Weather Review, 142(2), pp.905-921.

Satoh, M., Stevens, B., Judt, F., Khairoutdinov, M., Lin, S.J., Putman, W.M. and Düben, P., 2019. Global cloud-resolving models. Current Climate Change Reports, 5(3), pp.172-184.

Sillmann, J., Thorarinsdottir, T., Keenlyside, N., Schaller, N., Alexander, L.V., Hegerl, G., Seneviratne, S.I., Vautard, R., Zhang, X. and Zwiers, F.W., 2017. Understanding, modeling and predicting weather and climate extremes: Challenges and opportunities. Weather and climate extremes, 18, pp.65-74.

Skamarock, W.C., Klemp, J.B., Duda, M.G., Fowler, L.D., Park, S.H. and Ringler, T.D., 2012. A multiscale nonhydrostatic atmospheric model using centroidal Voronoi tesselations and C-grid staggering. Monthly Weather Review, 140(9), pp.3090-3105.

Skamarock, W.C., Park, S.H., Klemp, J.B. and Snyder, C., 2014. Atmospheric kinetic energy spectra from global high-resolution nonhydrostatic simulations. Journal of the Atmospheric Sciences, 71(11), pp.4369-4381.

Stevens, B., Satoh, M., Auger, L., Biercamp, J., Bretherton, C.S., Chen, X., Düben, P., Judt, F., Khairoutdinov, M., Klocke, D. and Kodama, C., 2019. DYAMOND: the DYnamics of the Atmospheric general circulation Modeled On Non-hydrostatic Domains. Progress in Earth and Planetary Science, 6(1), pp.1-17.

Stevens, B., Acquistapace, C., Hansen, A., Heinze, R., Klinger, C., Klocke, D., Rybka, H., Schubotz, W., Windmiller, J., Adamidis, P. and Arka, I., 2020. The added value of large-eddy and storm-resolving models for simulating clouds and precipitation. Journal of the Meteorological Society of Japan. Ser. II.

https://doi.org/10.5194/gmd-2022-111
Preprint. Discussion started: 17 June 2022

Geoscientific Model Development
Discussions

Zhao, C., Leung, L.R., Park, S.H., Hagos, S., Lu, J., Sakaguchi, K., Yoon, J., Harrop, B.E., Skamarock, W. and Duda, M.G., 2016. Exploring the impacts of physics and resolution on aqua-planet simulations from a nonhydrostatic global variable-resolution modeling framework. Journal of Advances in Modeling Earth Systems, 8(4), pp.1751-1768.